HHS Public Access

Author manuscript

Nat Immunol. Author manuscript; available in PMC 2017 January 25.

Published in final edited form as:

Nat Immunol. 2016 September ; 17(9): 1084–1092. doi:10.1038/ni.3512.

Apoptosis in response to microbial infection induces autoreactive T_H17 cells

Laura Campisi[1,3,†], **Gaetan Barbet**[1,3], **Yi Ding**[5], **Enric Esplugues**[6], **Richard A. Flavell**[6], and **J. Magarian Blander**[1,2,3,4,*]

[1]Immunology Institute, Icahn School of Medicine at Mount Sinai, New York, NY, USA

[2]Tisch Cancer Institute, Icahn School of Medicine at Mount Sinai, New York, NY, USA

[3]Department of Medicine, Icahn School of Medicine at Mount Sinai, New York, NY, USA

[4]Department of Microbiology, Icahn School of Medicine at Mount Sinai, New York, NY, USA

[5]Department of Pathology, New York University Langone Medical Center, New York, NY, USA

[6]Department of Immunobiology, Yale University School of Medicine, New Haven, CT, USA

Abstract

Microbial infections often precede the onset of autoimmunity. How infections trigger autoimmunity remains poorly understood. We investigated the possibility that infection might create conditions that allow the stimulatory presentation of self peptides themselves and that this might suffice to elicit autoreactive T cell responses that lead to autoimmunity. Self-reactive $CD4^+$ T cells are major drivers of autoimmune disease, but their activation is normally prevented through regulatory mechanisms that limit the immune-stimulatory presentation of self antigens. Here we found that the apoptosis of infected host cells enabled the presentation of self antigens by major histocompatibility complex class II molecules in an inflammatory context. This was sufficient for the generation of an autoreactive T_H17 subset of helper T cells, prominently associated with autoimmune disease. Once induced, the self-reactive T_H17 cells promoted auto-inflammation and autoantibody generation. Our findings have implications for how infections precipitate autoimmunity.

Autoimmunity is caused by pathogenic T and B cell responses directed against self[1-4]. Genetic background is the strongest predisposing factor, however, studies reporting disease discordance in identical twins and the large heterogeneity within a single disease[2,5] indicate

*Correspondence to: J. Magarian Blander, Julie.blander@mssm.edu.

†Present address: Department of Microbiology, Icahn School of Medicine at Mount Sinai, New York, NY USA and Global Health and Emerging Pathogens Institute, Icahn School of Medicine at Mount Sinai, New York, NY USA

AUTHOR CONTRIBUTIONS

L.C. and J.M.B designed and directed the study and wrote the manuscript. L.C. conducted all the experiments. G.B. assisted with T cell sorting experiments. Y.D. conducted the histological and pathological assessments on colonic tissues. E.E. and R.A.F. provided the IL-17eGFP reporter mice. J.M.B conceived of the study.

COMPETING FINANCIAL INTERESTS

The authors declare that they have no conflict of interest.

an additional role for environmental factors. Epidemiological studies have linked microbial infections and autoimmunity, suggesting that infections can trigger autoimmune diseases[6-9]. Several theories have been proposed including the bystander activation of autoreactive T cells by inflammation or pathogen-encoded super-antigens, as well as ‘epitope mimicry’ where self-reactive T cells are activated inappropriately by microbial peptides with homology to those from self[6,10]. Whether the response of innate immune cells to infection induces the activation of self-reactive adaptive responses is not known. Instead of invoking ‘epitope mimicry’, we investigated whether the presentation of self peptides themselves might be possible during certain infections and might result in the activation and subsequent differentiation of self-reactive T cells.

The presentation of self peptides by dendritic cells (DCs) in the context of inflammation and T cell co-stimulation is normally avoided and is thought to represent one mechanism of peripheral tolerance that prevents the priming of self-reactive T cells[11]. *In vitro* studies have shown that antigen presentation by bone-marrow-derived DCs (BMDCs) is regulated by Toll-like receptor (TLR) signals specifically from phagosomes containing pathogens and not from those containing apoptotic cells. This subcellular mechanism favors the presentation of microbial antigens over that of cellular antigens by major histocompat- ibility complex (MHC) class I and class II molecules[11,12]. However, phagocytosis of infected apoptotic cells delivers into the same phagosome both cellular and microbial antigens along with TLR ligands. Whether MHC class II (MHC-II) molecules present self and non-self-antigens within this scenario has never been investigated.

Here we found that during an infection that causes the apoptosis of infected colonic epithelial cells, self-reactive $CD4^+$ T cells with specificity to cellular antigens were activated along with $CD4^+$ T cells specific to the infecting pathogen. The self-reactive $CD4^+$ T cells differentiated into T_H17 cells, concordant with the inflammatory environment elicited by the combination of infection and apoptosis, which favors the development of a T_H17 response[13,14]. We found that the emergence of self-reactive T_H17 cells during colonic infection was associated with autoantibody production, along with enhanced susceptibility to intestinal inflammation. Our results have implications for understanding how microbial infection can elicit a break in tolerance and set the stage for the subsequent development of autoimmunity.

Results

MHC class II presentation of infected-apoptotic-cell antigen

Cellular antigens from apoptotic cells are presented by BMDCs only when those apoptotic cells concurrently contain a TLR ligand[11,12] (**Supplementary Fig. 1a**). Because phagocytosis of infected apoptotic cells would deliver TLR ligands along with cellular and microbial antigens to the same phagosome, we asked whether cellular antigen could be presented alongside microbial antigen in this scenario. We infected A20 B cells that express the α chain of I-E (Eα antigen) with recombinant *Listeria monocytogenes* expressing ovalbumin (LM-OVA), followed by induction of apoptosis with recombinant Fas ligand. Phagocytosis of LM-OVA infected, but not uninfected, apoptotic A20 cells by BMDCs derived from C57BL/6J (B6) mice, which do not express Eα, led to proliferation of both

1H3.1 and OT-II CD4$^+$ T cells (with transgenic expression of an Eα-specific T cell antigen receptor (TCR) and OVA-specific TCR, respectively) (**Supplementary Fig. 1b** and **Fig. 1a**). As expected, T cells proliferated to their respective cognate antigens derived from LM-OVA, recombinant OVA or Eα expressing *E. coli* or specific peptide pulsed onto BMDCs (**Fig. 1a**).

We next turned to orogastric infection with the rodent pathogen *Citrobacter rodentium*, which infects colonic intestinal epithelial cells and induces their apoptosis[13]. We generated bone marrow chimeric mice where lethally irradiated transgenic mice expressing a membrane bound form of OVA under the ubiquitous β-actin promoter (Act-mOVA) were reconstituted with donor bone marrow from CD11c-DTR mice expressing the diphtheria toxin (DT) receptor under the CD11c promoter (**Supplementary Fig. 1c**). As controls, we generated chimeric mice in which wild-type (WT) B6 mice served as recipients (**Supplementary Fig. 1c**). We adoptively co-transferred Vα2$^+$Vβ5$^+$ OT-II T cells, specific to the self-antigen OVA in this model (**Fig. 1b**, black bars) with 1H3.1 T cells (Vβ6$^+$) for which no cognate antigen is present (**Fig. 1b**, white bars). Both populations of T cells proliferated weakly after transfer, regardless of the presence or absence of cognate antigens and similar to levels in uninfected mice (**Fig. 1b**). However, proliferation of transferred OT-II T cells was markedly enhanced in Act-mOVA chimeric mice upon *Citrobacter* infection, and was driven by OVA as no such proliferation of 1H3.1 T cells was induced by infection. OT-II T cells no longer proliferated in response to infection upon DT depletion of CD11c$^+$ cells, or infection with ΔEspF *C. rodentium*, which lack the EPEC secreted protein (EspF) that mediates apoptosis[13] (**Fig. 1b**). As expected, 1H3.1 T cells did not proliferate under these conditions (**Fig. 1b**), but proliferated after injecting WT B6 mice with Eα-expressing *E. coli* (**Supplementary Fig. 1d)**. These data indicate that cellular antigen can be presented by CD11c$^+$ cells during *Citrobacter* infection, and in a manner dependent on the ability of infecting bacteria to induce apoptosis.

Pathogen-specific CD4$^+$ T cells induced by *C. rodentium* infection

Intestinal T$_H$17 responses are typically measured by antigen non-specific *ex-vivo* stimulation with PMA and ionomycin (**Fig. 2a** and **Supplementary Fig. 2a**). To examine the antigen specificities of the T$_H$17 CD4$^+$ T cell response in mice following *C. rodentium* infection, we stimulated CD4$^+$ T cells from the mesenteric lymph node (MLN) or large intestinal lamina propria (LI LP) with splenocytes pulsed with lysates from *C. rodentium* or control *Listeria monocytogenes*. Compared to stimulation with PMA–ionomycin, a considerably smaller percentage of CD4$^+$ T cells from infected mice responded by producing more IL-17 in response to *C. rodentium* compared to *L. monocytogenes* (**Fig. 2a** and **Supplementary Fig. 2a**). A fraction of *C. rodentium*-specific LI LP IL-17$^+$ CD4$^+$ T cells also produced IFN-γ and IL-22 (**Supplementary Fig. 2a**). IL-17$^+$CD4$^+$ T cells expressed the T$_H$17-specific transcription factor RORγt (**Fig. 2b**) and low levels of the T$_H$1-specific transcription factor T-bet, but not the regulatory T (T$_{reg}$) cell-specific transcription factor Foxp3, consistent with previous reports[15] (**Supplementary Fig. 2a,b**). After *ex vivo* re-stimulation, MLN CD4$^+$ T cells from infected mice secreted IL-17, IFN-γ and IL-22 in response to *C. rodentium* but not *L. monocytogenes* lysates (**Fig. 2c**). Consistent with other studies[16], colonic T$_H$17 cells did not produce IL-10 characteristic of regulatory T$_H$17 cells in

the small intestine[17,18] (**Supplementary Fig. 2c**). Instead, we noted decreased IL-10 production by $CD4^+$ T cells upon infection, which was confined to $Foxp3^+$ T_{reg} cells (**Supplementary Fig. 2c**).

Consistent with the T_H17 immune response being contingent upon infection-induced apoptosis of colonic epithelial cells[13,14], production of IL-17 by *Citrobacter*-specific LI LP $CD4^+$ T cells was impaired after infection with ΔEspF compared to WT *C. rodentium* (**Fig. 2d,e**), despite similar levels of T cell proliferation (**Fig. 2d**). Indeed, 50-60% of LI LP $CD4^+$ T cells proliferated in response to infection with either WT or ΔEspF *C. rodentium* compared to an average of 20% in uninfected mice, reflecting homeostatic T cell proliferation in response to the gut microbiota[19]. We also noted comparable shortening of the colons and similar fecal and colonic counts of WT or ΔEspF *C. rodentium* (**Supplementary Fig. 2d**), as previously reported[13]. Finally, upon *ex vivo* re-stimulation with bacterial lysate-pulsed splenocytes, IL-17 production by $CD4^+$ T cells was impaired in mice infected with ΔEspF compared to WT *C. rodentium*, but the amount of IFN-γ secretion was comparable (**Fig. 2e**). Accordingly, LI LP $CD4^+$ T cells expressed similar levels of T-bet upon infection with either bacterial strain, while RORγt was specifically expressed upon infection with WT but not ΔEspF *C. rodentium* (**Supplementary Fig. 2e**). Consistent with previous findings[20], the frequency of $Foxp3^+$ cells was reduced upon infection with either WT or ΔEspF *C. rodentium* (**Supplementary Fig. 2a,e**). Therefore, lack of apoptosis during infection does not affect $CD4^+$ T cell priming to *C. rodentium* antigens but rather impairs differentiation of *Citrobacter*-specific T_H17 cells.

Tracking self-reactive and pathogen-specific $CD4^+$ T cells

T_H17 cells mobilized upon infections causing apoptosis might harbor specificities not only to the infecting pathogen, but also to self-antigen from infected apoptotic cells. Unlike endogenous auto-reactive T cells, adoptively transferred T cells specific to a self-antigen in recipient mice (**Fig. 1b**) would not undergo central tolerance. To test whether apoptosis of infected cells could activate endogenous self-reactive T cells, we resorted to an experimental model typically used for natural T_{reg} enrichment where mice are transgenic for a TCR as well as its high affinity cognate antigen[21-23]. To this end, we crossed OT-II TCR to Act-mOVA transgenic mice (**Supplementary Fig. 3a**). Resultant offspring hereafter referred to as double transgenic (DTg) mice, harbored OTII $CD4^+$ T cells specific to OVA as a self-antigen. Consistent with previous studies[21-23], OVA-specific T cells in DTg mice underwent massive deletion but were still detectable in the thymus (~1% compared to ~95% in OT-II mice) (**Fig. 3a**), as well as in MLN (~5%) and large intestine (~8-10%) where a major polyclonal $CD4^+$ T cell population was also present reflecting transgenic TCRβ chain pairing with endogenous TCRα chains[24] (**Supplementary Fig. 3b,c**). OT-II $CD4^+$ T cells in secondary lymphoid organs of DTg mice were detected based on high expression of Vα2, to exclude T cells expressing endogenous TCRα chains[25], or by a specific tetramer of $I\text{-}A^b$ and peptide of OVA amino acids 328–337 (OVA(328–337)) ($I\text{-}A^b$–OVA(328-337)) showing their ability to bind cognate peptide presented on self MHC-II (**Supplementary Fig. 3b,c**). LI LP OTII $CD4^+$ T cells in both DTg and OT-II mice were $CD44^+$, consistent with the phenotype of intestinal $CD4^+$ T cells[26,27] (**Supplementary Fig. 3c**). Compared to MLN and LI LP OT-II T cells in single transgenic mice, OT-II T cells in DTg mice also expressed more CD5,

which correlates with TCR auto-reactivity[28] (**Fig. 3b**). Furthermore, $CD4^+$ T cells from OT-II mice stained more brightly upon detection with either I-A^b–OVA(328-337) or anti-Vβ5 than those from DTg mice (**Supplementary Fig. 3b,c**). This suggested that T cells with high avidity for IA^b–OVA(328-337) were eliminated in DTg mice, while those with low avidity remained, as previously reported[21-23]. Compared to single transgenic OT-II mice and concordant with a previous report[22], the thymus, MLN and LI LP in DTg mice were enriched in $Foxp3^+$ T_{reg} cells expressing the Vα2Vβ5 TCR (~28%, 18% and 40% **Fig. 3c,d**, respectively). Indeed, self-reactive $Vα2^{hi}Vβ5^+$ in the LI LP of DTg mice were enriched in $Foxp3^+$ T cells as compared to $Vα2^-Vβ5^-CD4^+$ T cells (**Fig. 3d**). $Vα2^{hi}Vβ5^+$OT-II T cells from DTg mice did not express detectable T-bet, GATA3 and RORγt (**Fig. 3e**).

Splenic $CD25^-CD4^+$ T cells from DTg mice underwent less proliferation than those from OT-II mice when stimulated *in vitro* with BMDCs pulsed with cognate OVA(323-339) peptide, despite the high concentration we used suggesting 'antigen tuning' of the self-reactive TCR[29] (**Fig. 3f)**. They also failed to secrete IL-17 consistent with their lack of RORγt expression (**Fig. 3e,g)**. These cells secreted IL-17 only when primed by BMDCs that had phagocytosed apoptotic TLR ligand$^+$$OVA^+$ B cells (**Fig. 3g**) consistent with T_H17 differentiation upon simultaneous DC recognition of TLR and apoptotic cell derived ligands[13,14].

Finally, despite the increased frequency of autoreactive $CD4^+$ T cells, DTg mice did not spontaneously develop autoimmunity and were healthy, as previously noted[22]. Compared to WT and single transgenic OT-II mice, DTg mice did not exhibit altered susceptibility to *C. rodentium* according to statistically insignificant differences in bacterial burdens and colitis scores after infection (**Supplementary Fig. 4a,b**). Additionally, the polyclonal LI LP T_H17 response after infection was comparable in DTg and Act-mOVA mice (**Supplementary Fig. 4c**). Thus, DTg mice are useful for studying autoreactive $CD4^+$ T cells during an infection that induces host cell apoptosis.

C. rodentium infection activates self-specific $CD4^+$ T cells

We next investigated whether *Citrobacter* infection known to induce apoptosis of colonic epithelial cells[13,14] could prime self-reactive $CD4^+$ T cells specific to cellular antigens derived from infected apoptotic cells. We observed a significant increase in the percentage of $BrdU^+Vα2^{hi}Vβ5^+CD4^+$ T cells in the LI LP after infection (~50%) compared to uninfected DTg mice (~30%) (**Fig. 4a**). Since *C. rodentium* infection preferentially induces T_H17 mediated immunity[14], we tested whether self-reactive $CD4^+$ T cells were also capable of acquiring this phenotype. Notably, ~15% of self-reactive $Vα2^{hi}Vβ5^+CD4^+$ T cells in the LI LP proliferated and produced IL-17 (**Fig. 4a**). We crossed DTg mice to IL17A-eGFP reporter mice (**Fig. 4b**) where eGFP was inserted in the *Il17a* locus[17], and tracked endogenous self-reactive $CD4^+$ T cells by tetramer staining. Consistently, the frequency of I-A^b–$OVA(328-337)^+$ $CD4^+$ T cells from DTg IL-17A reporter mice increased after infection compared to uninfected controls (~3 fold), and was specific as no similar increase was detected by staining for an irrelevant tetramer (**Fig. 4b**). Upon infection, I-A^b–$OVA(328-337)^+CD4^+$ T cells in Act-mOVA or OT-II mice did not express IL-17, while I-A^b–$OVA(328-337)^+CD4^+$ T cells in infected DTg mice contained an increased percentage of

IL-17-eGFP$^+$ cells as compared to uninfected DTg mice (~20% on average, right panels) (**Fig. 4b**). Self-reactive Vα2^{hi}Vβ5$^+$ cells expressed RORγt at levels comparable to those in non-self-reactive Vα2$^-$Vβ5$^-$ IL-17 producing CD4$^+$ T cells, but notably they did not express Foxp3, identifying these cells as *bona fide* T_H17 cells (**Fig. 4c**). Like total LI LP Foxp3$^+$CD4$^+$ T cells (**Supplementary Fig. 2c**), the percentage of self-reactive Foxp3$^+$Vα2^{hi}Vβ5$^+$ T_{reg} cells and their expression of IL-10 were reduced in infected DTg IL-10-eGFP reporter and DTg mice (**Supplementary Fig. 5a**).

Whereas MLN CD4$^+$ T cells from both Act-mOVA and DTg infected mice produced IL-17 in response to *Citrobacter* antigens *(Citrobacter*-specific response), only DTg mice contained a population secreting IL-17 in response to OVA(323-339) peptide-pulsed splenocytes (self-specific response) and not control peptide (**Fig. 4d**), confirming the induction of T_H17 cells specific to self-antigen in DTg mice. Interestingly, these cells did not secrete significant amounts of IFN-γ or IL-22 when compared to those from uninfected mice or those stimulated with noncognate peptide (**Fig. 4e**). On the other hand, LI LP *Citrobacter*-specific T_H17 cells secreted IL-22 and a subset of these cells acquired IFN-γ and T-bet expression (**Fig. 2c** and **Supplementary Fig. 2a,b**). This was also observed in *Citrobacter*-specific CD4$^+$ T cells purified from MLN of DTg mice (**Fig. 4e**). The types and levels of cytokines produced by *Citrobacter*-specific MLN CD4$^+$ T cells were similar in DTg and WT mice (compare **Fig. 2c** to **Fig. 4d,e**), demonstrating an intact *Citrobacter*-specific response (**Supplementary Fig. 4**). Collectively, these results show generation of a distinct self-reactive T_H17 response alongside a *Citrobacter*-specific T_H17 response after infection.

No antigen mimicry in self-specific CD4$^+$ T cell activation

The potential expression of a second TCR due to incomplete allelic exclusion of *Tcra* locus rearrangements[25] raised the possibility that self-reactive CD4$^+$ T cells might recognize a microbial antigen. We reconstituted irradiated CD45.1.2 Act-mOVA mice with bone marrow from CD45.2 OT-II *Tcra*$^{-/-}$ mice. Because such mice might be unable to cope with *C. rodentium* infection, chimeras also received bone marrow from CD45.1 WT mice at a 1:1 ratio (**Supplementary Fig. 5b**, schematic). Recipient mice expressed OVA as a self-antigen and contained CD45.1 CD4$^+$ T cells with a polyclonal TCR repertoire and CD45.2 CD4$^+$ T cells expressing a monoclonal Vα2Vβ5 TCR fixed on a *Tcra*$^{-/-}$ background (**Fig. 5a**). Low frequency of CD45.2 CD4$^+$ T cells in the LI LP and thymus (**Fig. 5a** and **Supplementary Fig. 5b**) indicated negative thymic selection, as reported in similar models[22]. Notably, *Citrobacter* infection induced IL-17 production not only by polyclonal CD45.1 CD4$^+$ T cells, but also by self-reactive CD45.2 OT-II *Tcra*$^{-/-}$ population (**Fig. 5a**). These data confirmed that the Vα2Vβ5 TCR, which is specific to OVA as a self-antigen in this model, and not another TCR comprised of Vβ5 paired with a different Vα, is responsible for the activation and differentiation of self-reactive T cells.

Infection-induced apoptosis drives self-reactive T_H 17 cells

If the source of self-antigen were indeed apoptotic cells, the absence of apoptosis should impair both proliferation and T_H17 differentiation of self-reactive CD4$^+$ T cells. Contrasting with mice infected with WT *C. rodentium*, self-reactive CD4$^+$ T cells failed to differentiate into T_H17 cells, and more importantly, were unable to proliferate in mice infected with the

ΔEspF *C. rodentium* that cannot induce apoptosis (**Fig. 5b**). Among $V\alpha2^{hi}V\beta5^{+}$ cells, the frequencies of proliferating cells were similar between uninfected and ΔEspF *Citrobacter* infected mice (**Fig. 5b**, right scatter plots). Blocking apoptosis during WT *Citrobacter* infection by treatment with a pan-caspase inhibitor that does not impact T cell activation[13], also impaired self-reactive $CD4^{+}$ T cell differentiation into T_H17 (**Supplementary Fig. 5c**). Blocking MHC-II presentation during infection with WT *C. rodentium* impaired the proliferation and IL-17 production by self-reactive $V\alpha2^{hi}V\beta5^{+}CD4^{+}$ T cells (**Fig. 5b**, WT +YP3 panels). These results show the need for antigen presentation in activating self-reactive $CD4^{+}$ T cells during infection-induced apoptosis.

Infection-associated auto-antibody secretion and colitis

Induction of T_H17 cells after colonization with segmented filamentous bacteria or infection with epithelial cell adherent bacteria[30], or after model oral vaccinations[31] and *C. rodentium* infection[13,30], are all accompanied with increased intestinal IgA. For autoimmune diseases including those of the gastrointestinal tract, autoantibodies are a key characteristic[4,32,33]. *Citrobacter* infection induced an increased level of serum anti-OVA IgA at day 40 after infection not observed in WT or single transgenic mice (**Fig. 6a**). Furthermore, using Act-mOVA mice as controls, we detected anti-OVA IgG1 in DTg infected mice, whereas natural anti-OVA IgM levels were comparable (**Supplementary Fig. 6a**). Anti-OVA IgA and IgG1 autoantibodies correlated with the presence of OVA-specific self-reactive T_H17 cells in DTg and not Act-mOVA mice (**Fig. 4a,b,d**), suggesting B cell help by T_H17 cells[33].

To address the role of autoreactive $CD4^{+}$ T cells in autoantibody secretion, we generated Act-mOVA chimeras reconstituted with bone marrow from WT Thy1.2 and OT-II Thy1.1 mice (**Supplementary Fig. 6b**, schematic) enabling specific depletion of OT-II T cells with anti-Thy1.1 before *C. rodentium* infection. Notably, OT-II T cell depletion abrogated the anti-OVA IgA response (**Fig. 6b**). On the other hand, serum anti-OVA IgM levels were similar in anti-Thy1.1 treated and untreated mice, consistent with the T-independent nature of the IgM response, while we could no longer detect serum anti-OVA IgG1 (**Supplementary Fig. 6c**). Thus, self-reactive T cells were responsible for the generation of class-switched IgA autoantibodies in this model.

Notably, 60% of DTg mice showed colonic neutrophilic and lymphocytic infiltration at day 40 post-infection with foci of aggregation suggesting a combined acute and chronic inflammatory process, whereas little to no pathology could be detected in WT, OT-II and ActmOVA (**Fig. 6c,d**). Different levels of epithelial hyperplasia and depletion of goblet cells were also observed (**Fig. 6c,d**). Large intestinal pathology in infected DTg mice was not due to an inability to clear bacteria (**Supplementary Fig. 4b**). A milder pathology was observed after depletion of Thy1.1 OT-II cells in chimeric mice (**Supplementary Fig. 6d).** Therefore, an enteric apoptosis-inducing infection has the potential to elicit intestinal pathology through the generation of a self-reactive T_H17 response (**Supplementary Fig. 6e,** model).

Discussion

Cumulative evidence has challenged the notion that clonal deletion purges the repertoire of self-reactive T cells[34,35]. Comparison of the frequency of self-reactive $CD4^{+}$ T cells within a

normal repertoire in mice lacking or expressing a defined self-antigen showed persistence of one-third of low-affinity self-reactive Foxp3$^+$ and Foxp3$^-$ CD4$^+$ T cells despite the presence of self-antigen[36]. Similar findings were reported for self-reactive CD8 T cells[37,38]. Autoreactive T cells have been detected in the peripheral blood of healthy individuals at frequencies similar to those in patients with autoimmune diseases[9,34,39]. In the context of autoimmune pathologies with stronger association to polymorphisms in MHC-II molecules (such as celiac disease), epidemiologic and genetic studies show that achieving a threshold number of autoreactive T cells is necessary for disease[40,41]. Genetic susceptibility to autoimmunity also includes anomalies in thymic selection and T cell signaling[1,42]. Increases in self-reactive cells and their progressive acquisition of an effector phenotype directly correlate with disease precipitation[40,41]. Nevertheless, the repertoire frequency of self-reactive T cells is small due to thymic deletion or inactivation[35,43], making it difficult to study and characterize these cells.

Transgenic expression of a TCR in a context where its cognate antigen is expressed as self leads to the generation of a low but detectable number of low-affinity self-reactive T cells that overcome thymic tolerance[21-23]. Using this experimental system, we show how infection contributes to the differentiation of autoreactive CD4$^+$ T cells into T_H17 cells associated with several autoimmune diseases[44-46]. By eliminating the possibility for self-reactive CD4$^+$ T cells to express TCRs other than the self-reactive TCR, we show that cognate self-antigen-TCR interaction is responsible for activation. In this same model, successful mobilization of a CD4$^+$ T cell response against *Citrobacter* infection demonstrates the preservation of a functional polyclonal T cell repertoire. During an infection that causes host cell apoptosis, the instruction of T_H17 fate in CD4$^+$ T cells is a consequence of innate recognition of infected apoptotic cells, which promotes DC production of TGF-β (to apoptotic cell induced phosphatidyl serine) and IL-6 (to TLR ligands from the infection)[13,14]. Upon phagocytosis of infected apoptotic cells, the simultaneous phagosomal compartmentalization of apoptotic cells and microbial cargo expressing TLR ligands optimally tailors those phagosomes for antigen presentation[11], providing equal opportunity for both self and non-self-peptides to be loaded onto MHC-II molecules.

Citrobacter induces apoptosis as the specific mode of colonic intestinal epithelial cell death, and the T_H17 response is highly impaired in mice infected with ΔEspF *Citrobacter* that cannot induce apoptosis[13,14]. Necrosis or pyroptosis may not instruct T_H17 differentiation mainly because of their inability to induce simultaneous DC secretion of biologically active TGF-β and inflammatory cytokines by DCs[13,14]. Although NLRP3-dependent pyroptosis has been reported in response to *C. rodentium* and irrespective of some locus of enterocyte effacement pathogenicity island effectors[47], the lack of self-reactive CD4$^+$ T cell activation upon ΔEspF *Citrobacter* infection argues against a role for pyroptosis in releasing intact self-antigens or driving bystander activation of self-reactive CD4$^+$ T cells. Furthermore, the latter cannot be driven by infection-induced inflammation *per se* as evidenced by impaired self-reactive CD4$^+$ T cell activation upon MHC-II blockade.

Self-reactive T cells are controlled by peripheral Foxp3$^+$ T_{reg} cells[39]. Indeed, autoimmune disease in mice and humans lacking Foxp3$^+$CD4$^+$ T cells is strong evidence for the presence

of self-reactive $CD4^+$ T cells within the normal T cell repertoire[22]. Systemic T_{reg} cell ablation mediates the activation of $CD4^+$ T cells with specificity to select tissue-restricted self-antigens upon cognate peptide immunization[48]. Intact peripheral tolerance may explain the healthy status of our DTg mice, the absence of an effector phenotype among self-reactive $CD4^+$ T cells at steady state, as well as the moderate intestinal pathology elicited after an infection that induces apoptosis. On the other hand, a decrease in IL-10 and $Foxp3^+CD4^+$ T cells after *Citrobacter* infection in both DTg and WT animals, as reported previously[20], may enable the mobilization of an anti-bacterial T_H17 response and additionally contribute to the activation of self-reactive T cells in our model. One proposed mechanism for the decrease in $Foxp3^+CD4^+$ T cells is that secretion of IL-1 during *Citrobacter* infection favors T_H17 over T_{reg} cell differentiation during infection[20].

Microbes adhering to intestinal epithelial cells induce both T_H17 cell differentiation and IgA secretion[30], as also shown for *Citrobacter*[13,30]. Intriguingly, we also noted a link between self-reactive T_H17 cell differentiation and IgA production whereby self-reactive IgA produced in response to *Citrobacter* infection was abrogated upon deletion of self-reactive $CD4^+$ T cells. Self-reactive T_H17 cells might migrate to germinal centers in the large intestine to interact with B cells and facilitate IgA class-switching[49]. The increased susceptibility of DTg mice to colitis was also ameliorated upon depletion of self-reactive $CD4^+$ T cells suggesting a role for self-reactive T_H17 cells in the development of colitis. Indeed, increased IgA and T_H17 responses have both been associated with inflammatory bowel diseases albeit in the context of microbe recognition[30,50]. The colitis observed here was mild likely because auto-aggression by self-reactive T cells would culminate in full-blown autoimmunity only in the setting of polymorphisms for multiple genes involved in immune tolerance and function, and consistent with the multifactorial etiology of autoimmune diseases[1]. Finally, the link between infection and autoreactive T cell activation supports the idea that pathogen tropism could determine the specific localization of autoimmune diseases, despite ubiquitous expression of self-antigens[2]. Thus, our study provides a mechanism for how infection might trigger autoimmune disease in genetically susceptible individuals and has implications for new therapeutic avenues to limit disease precipitation.

ONLINE METHODS

Mice and various mouse related methods

C57Bl/6J, C57BL/6.Ly5.1 (CD45.1), Act-mOVA (C57BL/6-Tg(CAG-OVA)916Jen/J), OT-II (B6.Cg-Tg(TcraTcrb)425Cbn/J), IL-10-eGFP (B6.129S6-*Il10tm1Flv*/J), CD11c-DTR/GFP and $Tcra^{-/-}$ mice were purchased from The Jackson Laboratories. These strains and combinations thereof were bred in our mouse facility. IL17A-eGFP × FoxP3-mRFP mice were previously described[17]. 1H3.1 mice were previously described[51].

Chimeric mice were generated after two rounds of lethal irradiation with 600 Rads. Twenty-four later, irradiated mice were reconstituted by intravenous injection of $1\text{-}4\times10^6$ T cell-depleted bone marrow cells isolated from different strains of mice indicated in the text. T cells were depleted by incubation with an anti-CD3ε (clone 145-2C11, Biolegend) phycoerythrin (PE)-conjugated antibody, followed by anti-PE magnetic microbeads positive

selection (Miltenyi biotec), according to the manufacturer's instructions. Cells in the flow through were counted and injected into irradiated mice. For mixed bone marrow chimeric mice, we used a ratio of 1:1 of cells as indicated in the text. Chimeric mice were studied 8 weeks after bone marrow transplantation.

For the anti-I-A^b treatments, monoclonal antibody YP3 was purchased from Bio X Cell. Mice were injected intraperitoneally with 0.5 mg of antibody 2 hours before and after infection, and with 1 mg at 24, 48 and 72 hours post-infection. Anti-Thy1.1 monoclonal antibody (clone 19E12, Bio X Cell) was injected intraperitoneally at the dose of 0.5 mg 24 hours before infection. 0.4 mg of Q-VD-OPH (SM Biochemicals) were injected intraperitoneally at 90 min, 24 and 48 hours post-infection.

To deplete $CD11c^+$ cells, CD11c-DTR or chimeric mice reconstituted with CD11c-DTR bone marrow cells were injected intraperitoneally with 4ng/g of weight with diphtheria toxin (DT, Calbiochem) in PBS 24 hours before infection and daily after infection.

All mice were kept under specific pathogen-free conditions in the animal care facility at the Icahn School of Medicine at Mount Sinai (ISMMS). Both male and female mice were studied at 6–12 weeks of age. For experiments involving comparisons among OT-II, Act-mOVA and DTg mice only littermates were used. For experiments involving comparisons among chimeras, mice with different genotypes and/or bone marrow donors were co-housed after irradiation and throughout the study. In all experiments, mice were randomly assigned to the different groups (uninfected, infected, treated and untreated). All groups of mice included both males and females in comparable numbers and were processed identically throughout the whole experiment (housed on the same shelf in the same room, and all procedures performed at the same time). Investigators were not blinded for this study, except for the histological analysis (see “Microscopic Examination of Colons” section).

Animal numbers were empirically determined as the minimum needed to obtain statistical significance and validate reproducibility, accordingly with our IACUC approved protocol. All experiments were approved by the institutional animal care and use committee and carried out in accordance with the ‘Guide for the Care and Use of Laboratory Animals’ (NIH publication 86-23, revised 1985).

Bacteria and infection of mice

After 6 hours of starvation, mice were orogastrically infected with 10^9 and 10^{10} wild-type or ΔEspF *Citrobacter rodentium* (strains DBS100), respectively. ΔEspF *Citrobacter rodentium* is known to induce apoptosis of infected target cells[13,52-54]. We rendered these strains resistant to chloramphenicol by bacterial conjugation using the plasmid pMAC5 containing the mini Tn7 transposon that inserted the antibiotic resistance downstream of the *glmS* gene[55], as previously described[56,57]. Briefly, pMAC5 was electroporated into MFDpir bacteria followed by a tri-parental mating with MFDpir expressing pMAC5 + MFDpir expressing pTNS2 + *C. rodentium* DBS100, where the pTNS2 plasmid had the *tnsABCD* encoding for the Tn*7* transposase. Neither pMAC5 nor pTNS2 plasmids can replicate in *C. rodentium*. Conjugation was performed overnight in lysogeny broth (LB) medium supplemented with diaminopimelic acid (DAP, Sigma), necessary for the growth of the

MFDpir strain. Chloramphenicol resistant DBS100 where transposition occurred were then counter-selected in presence of the antibiotic and in absence of DAP to eliminate MFDpir bacteria. For experiments, bacteria were grown to exponential phase in LB medium supplemented with chloramphenicol (20 μg/ml), then washed and resuspended in 200 μL of phosphate-buffered saline (PBS) prior to gavage. To determine *C. rodentium* burdens in the stool or colon, stools and colons were weighed, homogenized in water, plated in MacConkey agar plates supplemented with chloramphenicol (20 μg/mL), and pink colonies were counted after incubation for 24 hours at 37°C. Bacterial colony forming units (CFU) were normalized to stool and colon weight.

Recombinant *E. coli* expressing a Curlin-Eα fusion protein, previously described[11,12], was prepared by growing *E. coli* to an optical density at 600 nm (OD_{600}) of 0.6 and adding 0.2 mM IPTG (for induction of fusion proteins) for an additional 6 hours of culture. Bacteria were then diluted in PBS to OD_{600}, killed by heating at 60°C for 1 hour. 10^9 heat-killed bacteria were then resuspended in PBS and injected intravenously into mice that had previously been anesthetized by isoflurane inhalation.

Cell isolation

Isolation of Lamina propria lymphocytes (LPL)—Lamina propria lymphocytes (LPL) were isolated from the large intestine, as previously described[13] with some modifications. Briefly, fragments of intestines were flushed with PBS, cut longitudinally, placed in 50 mL conical tubes, and washed several times in PBS by vortexing at maximum setting for 15-20 seconds. Tissues were then removed and placed in 50 mL conical tubes containing 25 mL of RPMI (Sigma), 5% fetal bovine serum (FBS) (Sigma), 1 mM DTT and 3 mM EDTA, then placed on a rocker at 37°C for 35 minutes followed by vortexing extensively at maximum setting. After PBS washing, cells were successively transferred in 7 mL of RPMI, 5% FBS, 1.6 mg/mL collagenase D (Roche), 20 μg/mL DNase (Roche), cut into small pieces and incubated for one hour on a rocker at 37°C before homogenization using a 20g syringe. Tissue suspensions were then filtered through a 70 μm cells strainer (BD Falcon), pelleted, resuspended in a 40% isotonic Percoll solution (GE Healthcare), and underlaid with an 80% isotonic Percoll solution. After 20 minutes of centrifugation at 2,800 rpm, mononuclear cells were recovered at the 40 – 80% interface and washed.

Preparation of single cell suspensions from the thymus, spleen, lymph nodes (LNs) and bone marrow—Single cell suspensions were prepared from the thymus, spleen, and mesenteric lymph nodes (MLNs) by pressing the tissues through a 70 μm cell strainer followed by homogenization using a 20g syringe and from the bone marrow by flushing the long bones with PBS.

Ex-*vivo* re-stimulation after primary stimulation *in vivo* with *Citrobacter* infection

For non-antigen specific re-stimulation, cells were resuspended in complete (*i.e.* supplemented with 10% FBS, 100 μg/mL penicillin, 100 μg/mL streptomycin, 2 mM L-glutamine, 10 mM HEPES, and 1 nM sodium pyruvate) IMDM (Sigma) with 0.1 μg/mL Phorbol 12-myristate 13-acetate (PMA, Sigma), 0.5 μg/mL ionomycin calcium salt, from

Streptomyces conglobatus (Sigma), and 10 μg/mL Brefeldin A, from *Eupenicillium brefeldanium* (Sigma), and incubated for 4-6 hours at 37°C.

For antigen-specific re-stimulation, splenocytes from C57BL/6J CD45.1 mice were used as antigen presenting cells (APC) after $CD3^+$ T cell depletion by incubation with anti-CD3 PE-conjugated antibody, followed by anti-PE magnetic microbeads positive selection (Miltenyi biotec), according to the manufacturer's protocol. Cells from the flow-through were counted, resuspended at 10^7 cells/mL in complete IMDM and incubated with 200 μg of *Citrobacter rodentium* or *Listeria monocytogenes* lysates, or 10 μg/mL of the peptides as indicated in the article text and figure legends. APC were plated in 96 round bottom at 5×10^5 cells/well for LPL or 1×10^6 cells/well for MLN cells, and incubated for 1-2 hours at 37°C.

For intracellular staining, LPL and MLN cells were added to culture in the presence of 10 μg/mL Brefeldin A for an additional 6 hours. For cytokine quantification by ELISA, $CD4^+$ T cells from MLN were purified by negative selection using Dynal Mouse CD4 Negative selection kit (Invitrogen Dynal) and plated at 2×10^6 cells/well with antigen-pulsed APC. Supernatants were collected for analysis at 48 hours.

For isolation of $CD4^+$ T cells for adoptive transfer or *in vitro* antigen presentation assays, splenocytes from OT-II or 1H3.1 mice were incubated with anti-CD4 magnetic microbeads for $CD4^+$ T cell positive selection (Miltenyi biotec), according to the manufacturer's instructions. A mixture of 5×10^5 OT-II and 5×10^5 1H3.1 $CD4^+$ T cells was adoptively transferred into the chimeric mice indicated in the text.

Antigens

To prepare bacterial lysates, wild-type (WT) *C. rodentium* (strain DBS100) and ΔLLO *ΔflaA L. monocytogenes* (strain 10403s, double deficient for Listeriolysin O and flagellin) were cultured in LB and brain heart infusion (BHI) broth, respectively, until exponential phase, then washed several times in PBS to eliminate medium. After resuspension in 1mL PBS + protease inhibitors (Roche), bacteria were sonicated on ice, then centrifuged 30 minutes at 13000 rpm. Supernatants were collected and filtered using membrane filters with 0.2 μm pore size (Millipore). Protein concentrations were determined using the Bradford Protein Assay (Bio-Rad). OT-II peptide, OVA(323-339) (sequence ISQAVHAAHAEINEAGR) was purchased from the Proteomics Resource Center of The Rockefeller University. GFP(26-39) (sequence HDFFKSAMPEGYVQE) and Eα(52-68) (sequence ASFEAQGALANIAVDKA) peptides were purchased from Abgent.

Antibodies, tetramers, 5-Bromo-2'-deoxyuridine (BrdU) and CFSE labeling

For flow cytometry, the following antibodies were purchased from eBioscience and were all used at a 1:100 dilution: anti-mouse CD45.1 (clone A20), CD4 (clone RM4-5), CD44 (clone IM7), Vα2 (clone B20.1), CD5 (clone 53-7.3), CD25 (clone PC61.5), CD8β (clone eBioH35-17.2), CD16/32 (clone 93), Thy 1.1 (clone HIS51), TCRβ (clone H57-597), IL17A (clone eBio17B7), IFN-γ (clone XMG1.2), Foxp3 (clone FJK-16s), RORγt (clone B2D), and T-bet (clone 4B10). We purchased from Biolegend: anti-mouse CD45.2 (clone 104), CD45 (clone 30-F11), CD3ε (clone 145-2C11), B220 (clone RA3-6B2), IL-22 (clone Poly5164). The anti-mouse Vβ5.1/5.2 TCR (clone MR9-4) was obtained from BD

Bioscience. An anti-GFP rabbit polyclonal antibody (Life technologies) was used for intracellular staining in cells purified from IL-10-eGFP and IL17A-eGFP×FoxP3-mRFP. Dead cells were discriminated in all experiments using LIVE/DEAD Fixable Aqua Dead Cell stain kit (Molecular Probes by Life technologies, used at 1:1000). PE or APC-conjugated I-A^b–HAAHAEINEA tetramer was used to stain OT-II CD4 T cells[28] and I-A^b–PVSKMRMATPLLMQA tetramer was used as a negative control. Both tetramers were provided by the NIH Tetramer Core Facility and used at a concentration of 20 μg/mL.

For surface staining, cells were suspended in PBS, 2% FBS, anti-mouse CD16/32, 2% mouse serum (Jackson laboratories), 2% rat serum (Jackson laboratories) and 0.1% NaN_3. For intracellular staining, cells were fixed in Fixation/Permeabilization buffer (eBioscience) and stained in Perm/Wash buffer (eBioscience).

For the *in vivo* proliferation experiments, mice were injected daily intraperitoneally with 1 mg of 5-Bromo-2'-deoxyuridine (Sigma) starting from day 1 after infection. BrdU Flow kit (BD Pharmingen) was used to detect intracellular BrdU incorporation according to the manufacturer's instructions. For carboxyfluorescein diacetate succinimidyl ester (CFSE) labeling, cells were resuspended at $2x10^6$ cells/well in PBS with 5 μM CFSE (eBioscience) for 10 minutes at 37°C and then washed.

Acquisition of stained cells was made with a BD LSRFortessa flow cytometer (BD Bioscience) and data were analyzed with FlowJo software (Treestar).

Enzyme-linked immunoabsorbent assays (ELISA)

Supernatants from cell cultures were collected at the times indicated for each experiment in the figure legends. The following ELISA monoclonal Ab (mAb) pairs were used: anti-mouse IL-17 (clones TC11-18H10/TC11-8H4.1, BD Biosciences) and IFN-γ (AN-18/R4-6A2, BD Biosciences). All antibodies were used at 1.5 μg/mL for capture and detection. The recombinant cytokines used as standards were purchased from Peprotech. Detection antibodies were all biotinylated. Streptavidin-conjugated horseradish peroxidase (HRP) was added and visualized by *o*-phenylenediamine dihydrochloride (SIGMA) (from tablets) or 3,3', 5,5'-tetramethylbenzidine solution (TMB, KPL). IL-22 was measured using the Quantikine®ELISA mouse/rat IL-22 kit. Supernatants were incubated undiluted or diluted in polystyrene microtiter plates (Nunc), except for IL-22 ELISA where the plate was included in the kit. Absorbances at 490nm or 450nm were measured using a tunable microplate reader (VersaMax, Molecular Devices). Cytokine supernatant concentrations were calculated by extrapolating absorbance values from standard curves where known concentrations were plotted against absorbance using SoftMax Pro 5 software.

Serum immunoglobulin titer measurements

Mice were anesthetized by isoflurane inhalation and then bled retroorbitally using heparinized micro-hematocrit capillary tubes (Fisherbrand). Twenty to fifty μl of blood were collected in 1 ml eppendorff tubes and centrifuged for 10 min at 10,000 rpm to separate the serum. Serum immunoglobulin titers were measured by ELISA. Polystyrene microtiter plates (Nunc) were coated overnight with 50 μg/ml of ovalbumin (OVA) protein (Sigma), then washed and blocked with bovine serum albumin (1%). Serum samples were applied at

1:5 dilution, and incubated for 3 hours at room temperature, then washed and incubated with alkaline-phosphatase-goat-anti-mouse IgM, IgA, IgG1 (1:100) developed by the addition of *p*-nitrophenyl phosphate solution (Sigma-Aldrich). Optical density (OD) 490 nm was measured using a Molecular Devices spectrophotometer.

In vitro antigen presentation assays

Bone marrow (BM)-derived GM-CSF DC cultures were grown in 24 well plates as previously described[11,13] in RPMI supplemented with GM-CSF and 5% FBS, plus 100 μg/mL penicillin, 100 μg/mL streptomycin, 2 mM L-glutamine, 10 mM HEPES, 1 nM sodium pyruvate, 1X MEM nonessential amino acids, and 2.5 μM β-mercaptoethanol (all SIGMA). Different phagocytic cargo as indicated below or peptides were added to the culture on day 5. OVA(329-337) and Eα(52-68) peptides were added at 1μg/ml.

Phagocytic cargo—For experiments with bacteria, recombinant OVA-expressing *Listeria monocytogenes* (LM-OVA) were cultured in BHI medium until exponential phase, then washed several times in PBS to eliminate medium. Before addition to BMDC, LM-OVA were killed by incubation for 2 hours at 37°C in PBS containing 50 μL of Ampicillin. Recombinant *E. coli* expressing a flagellin-ovalbumin or Curlin-Eα fusion protein (*E. coli*-OVA and *E.coli*-Eα, respectively), previously described[11,12], were prepared by growing *E. coli* to an optical density at 600 nm (OD_{600}) of 0.6 and adding 0.2 mM IPTG (for induction of fusion proteins) for an additional 6 hours of culture. Bacteria were then diluted in PBS to OD_{600}, and then killed by heating at 60°C for 1 hour. All bacterial cargo were added to BMDC at a ratio of 1:100 (DC:bacteria) for 6 hours before T cells were added. For experiments with apoptotic cells, the A20 B cell line was obtained from the ATCC and splenic B cells from Act-mOVA BALB/c mice were purified using the anti-CD19 magnetic microbeads for B cell positive selection (Miltenyi biotec), according to the manufacturer's instructions. The A20 B cell line was confirmed to be mycoplasma free. A20 and B cells were cultured in RPMI medium (Sigma), supplemented with 10% FBS, 100 μg/mL penicillin, 100 μg/mL streptomycin, 2 mM L-glutamine, 10 mM HEPES, and 1 nM sodium pyruvate. Cells used in this study were not contaminated by mycoplasma. Apoptosis was induced by culturing with 0.5 μL anti-CD95 (clone Jo2; BD Biosciences) for 2 hours (A20 cells) or by UV irradiation at 350 mJ (B cells). For experiments with infected apoptotic cells, LM-OVA bacteria were cultured until exponential phase, then washed and incubated with A20 cells at MOI=100 for 8 hours. 50 μg/mL of Ampicillin (to kill all the bacteria) and anti-CD95 were then added to the culture for an additional 2 hours. LPS-B cell blasts were generated by adding to the cell culture 25 μg/mL LPS (from *Escherichia coli*, serotype 055:B5, L-2880, SIGMA). Infected A20 cells and LPS blasts were washed 3 times in PBS, and then added to BMDC cultures. Both uninfected and infected apoptotic cargo were added to BMDC at a ratio of 1:2 (DC:apoptotic cells) for 8 hours before adding CD4 T cells.

$CD4^+$ T cells—$CD4^+$ T cells were purified as described above, were incubated for 10 minutes at 37°C with 2.5 μM CFSE in PBS, washed, then suspended in IMDM complete medium and co-cultured with BMDC for 5 days.

Microscopic Examination of Colons

For histological analyses, the colons were removed, cut open along the lengths and fixed in 10% formalin overnight. Emdedding in paraffin blocks and staining with H&E were conducted by the Biorepository and Pathology Dean's CoRE at the ISMMS and untreated mice were used as controls. Microscopic sections were analyzed in a blinded fashion by the same pathologist (Y. Ding, M.D. Ph.D.). Briefly, a number was randomly assigned by the investigator to discriminate each section, which was then submitted for analysis as “section 1”, “section 2”, etc. No information about treatments and mouse genotypes was communicated to the pathologist.

Colons were graded semi-quantitatively as 0 (no change) to 4 (most severe) for the following inflammatory lesions: severity of chronic inflammation, crypt abscesses, and granulomatous inflammation; and for the following epithelial lesions: hyperplasia, mucin depletion, ulceration, and crypt loss. Results were expressed as the mean of the grades + standard deviation of affected mice. In addition, the depth of the inflammatory process into the large intestinal wall was categorized as extending into the mucosa, the submucosa, or the tunica muscularis or as being transmural (extending to the serosa)[58,59].

Statistical analysis

Statistical analyses were performed using GraphPad Prism. We first calculated the Gaussian distribution of the data using the Kolmogorov-Smirnov test. When two groups were compared, t-test (Gaussian distribution) and Mann-Whitney test (no Gaussian distribution) were used. When several groups were compared, we used a One-way ANOVA test followed by Tukey (Gaussian distribution) or Dunnet (no Gaussian distribution) post-hoc tests. $P \leq 0.05$ were considered significant. *P*-values are depicted in the figure legends with corresponding symbols on the graphical data, NS= not significant ($P > 0.05$).

Supplementary Material

Refer to Web version on PubMed Central for supplementary material.

ACKNOWLEDGEMENTS

We thank S. Lira, G. Furtado, H. Xiong, G. Yeretssian, M.K. Jenkins and members of the Blander laboratory for discussions; D. Amsen and R.J. Cummings for critical reading of the manuscript; A. Rialdi for help with statistical analyses; J. Ochando and C. Bare for flow cytometry; A. Soto and M.J. Suarez (the NIH Tetramer Core Facility at Emory University) for I-Ab–OVA(328–337) and control tetramers; H. Xiong (The Icahn School of Medicine at Mount Sinai) for LM-OVA bacteria; A. Morelli (University of Pittsburgh) for 1H3.1 mice; B. Finlay and M. Croxen (University of British Columbia) for wild-type and ΔEspF C. rodentium and plasmid pMAC5; H.P. Schweizer (Colorado State University) for plasmid pTNS2; D. Mazel (Institut Pasteur) for MFDpir bacteria; and I. Marazzi, V. Verhasselt, S.E.F. Campisi, G.C. Chiesa, Jr., M.A. Blander, S.J. Blander and the late L. Mayer for advice and support. Supported by the National Institute of Diabetes and Digestive and Kidney Diseases (DK072201 to J.M.B.), the National Institute of Allergy and Infectious Diseases (AI073899, AI080959 and AI095245 to J.M.B.), the Arthritis Foundation (L.C.), the Crohn’s and Colitis Foundation of America (G.B.), the Burroughs Wellcome Fund (J.M.B.), the Irma Hirschl and Monique Weill-Caulier Charitable Trust Funds (J.M.B.), the American Cancer Society (J.M.B.) and the Leukemia and Lymphoma Society (J.M.B.).

References

1. Cho JH, Gregersen PK. Genomics and the multifactorial nature of human autoimmune disease. The New England journal of medicine. 2011; 365:1612–1623. [PubMed: 22029983]

2. Marrack P, Kappler J, Kotzin BL. Autoimmune disease: why and where it occurs. Nat Med. 2001; 7:899–905. [PubMed: 11479621]

3. Sakaguchi S, Powrie F, Ransohoff RM. Re-establishing immunological self- tolerance in autoimmune disease. Nat Med. 2012; 18:54–58. [PubMed: 22227673]

4. Suurmond J, Diamond B. Autoantibodies in systemic autoimmune diseases: specificity and pathogenicity. J Clin Invest. 2015; 125:2194–2202. [PubMed: 25938780]

5. Cho JH, Feldman M. Heterogeneity of autoimmune diseases: pathophysiologic insights from genetics and implications for new therapies. Nat Med. 2015; 21:730–738. [PubMed: 26121193]

6. Blander JM, Torchinsky MB, Campisi L. Revisiting the old link between infection and autoimmune disease with commensals and T helper 17 cells. Immunologic research. 2012; 54:50–68. [PubMed: 22460741]

7. Pordeus V, Szyper-Kravitz M, Levy RA, Vaz NM, Shoenfeld Y. Infections and autoimmunity: a panorama. Clin Rev Allergy Immunol. 2008; 34:283–299. [PubMed: 18231878]

8. Sfriso P, et al. Infections and autoimmunity: the multifaceted relationship. J Leukoc Biol. 2010; 87:385–395. [PubMed: 20015961]

9. Rosenblum MD, Remedios KA, Abbas AK. Mechanisms of human autoimmunity. J Clin Invest. 2015; 125:2228–2233. [PubMed: 25893595]

10. Root-Bernstein R, Fairweather D. Complexities in the relationship between infection and autoimmunity. Curr Allergy Asthma Rep. 2014; 14:407. [PubMed: 24352912]

11. Blander JM, Medzhitov R. Toll-dependent selection of microbial antigens for presentation by dendritic cells. Nature. 2006; 440:808–812. [PubMed: 16489357]

12. Nair-Gupta P, et al. TLR Signals Induce Phagosomal MHC-I Delivery from the Endosomal Recycling Compartment to Allow Cross-Presentation. Cell. 2014; 158:506–521. [PubMed: 25083866]

13. Torchinsky MB, Garaude J, Martin AP, Blander JM. Innate immune recognition of infected apoptotic cells directs T(H)17 cell differentiation. Nature. 2009; 458:78–82. [PubMed: 19262671]

14. Brereton CF, Blander JM. The unexpected link between infection-induced apoptosis and a TH17 immune response. J Leukoc Biol. 2011; 89:565–576. [PubMed: 21248151]

15. Hirota K, et al. Fate mapping of IL-17-producing T cells in inflammatory responses. Nat Immunol. 2011; 12:255–263. [PubMed: 21278737]

16. Mowat AM, Agace WW. Regional specialization within the intestinal immune system. Nature reviews. Immunology. 2014; 14:667–685.

17. Esplugues E, et al. Control of TH17 cells occurs in the small intestine. Nature. 2011; 475:514–518. [PubMed: 21765430]

18. McGeachy MJ, et al. TGF-beta and IL-6 drive the production of IL-17 and IL-10 by T cells and restrain T(H)-17 cell-mediated pathology. Nat Immunol. 2007; 8:1390–1397. [PubMed: 17994024]

19. Berer K, et al. Commensal microbiota and myelin autoantigen cooperate to trigger autoimmune demyelination. Nature. 2011; 479:538–541. [PubMed: 22031325]

20. Basu R, et al. IL-1 signaling modulates activation of STAT transcription factors to antagonize retinoic acid signaling and control the TH17 cell-iTreg cell balance. Nat Immunol. 2015; 16:286–295. [PubMed: 25642823]

21. Marks BR, et al. Thymic self-reactivity selects natural interleukin 17-producing T cells that can regulate peripheral inflammation. Nat Immunol. 2009; 10:1125–1132. [PubMed: 19734905]

22. Simons DM, et al. How specificity for self-peptides shapes the development and function of regulatory T cells. J Leukoc Biol. 2010; 88:1099–1107. [PubMed: 20495071]

23. Zehn D, Bevan MJ. T cells with low avidity for a tissue-restricted antigen routinely evade central and peripheral tolerance and cause autoimmunity. Immunity. 2006; 25:261–270. [PubMed: 16879996]

24. Malissen M, et al. Regulation of TCR alpha and beta gene allelic exclusion during T-cell development. Immunol Today. 1992; 13:315–322. [PubMed: 1324691]

25. Padovan E, et al. Expression of two T cell receptor alpha chains: dual receptor T cells. Science. 1993; 262:422–424. [PubMed: 8211163]

26. Jalkanen S, Nash GS, De los Toyos J, MacDermott RP, Butcher EC. Human lamina propria lymphocytes bear homing receptors and bind selectively to mucosal lymphoid high endothelium. European journal of immunology. 1989; 19:63–68. [PubMed: 2465905]
27. Shimizu Y, Van Seventer GA, Siraganian R, Wahl L, Shaw S. Dual role of the CD44 molecule in T cell adhesion and activation. J Immunol. 1989; 143:2457–2463. [PubMed: 2677141]
28. Mandl JN, Monteiro JP, Vrisekoop N, Germain RN. T cell-positive selection uses self-ligand binding strength to optimize repertoire recognition of foreign antigens. Immunity. 2013; 38:263–274. [PubMed: 23290521]
29. Grossman Z, Paul WE. Autoreactivity, dynamic tuning and selectivity. Current opinion in immunology. 2001; 13:687–698. [PubMed: 11677091]
30. Atarashi K, et al. Th17 Cell Induction by Adhesion of Microbes to Intestinal Epithelial Cells. Cell. 2015; 163:367–380. [PubMed: 26411289]
31. Fonseca DM, et al. Microbiota-Dependent Sequelae of Acute Infection Compromise Tissue-Specific Immunity. Cell. 2015; 163:354–366. [PubMed: 26451485]
32. Di Sabatino A, Lenti MV, Giuffrida P, Vanoli A, Corazza GR. New insights into immune mechanisms underlying autoimmune diseases of the gastrointestinal tract. Autoimmun Rev. 2015
33. Sweet RA, Lee SK, Vinuesa CG. Developing connections amongst key cytokines and dysregulated germinal centers in autoimmunity. Current opinion in immunology. 2012; 24:658–664. [PubMed: 23123277]
34. Richards DM, Kyewski B, Feuerer M. Re-examining the Nature and Function of Self-Reactive T cells. Trends Immunol. 2016; 37:114–125. [PubMed: 26795134]
35. Hogquist KA, Jameson SC. The self-obsession of T cells: how TCR signaling thresholds affect fate 'decisions' and effector function. Nat Immunol. 2014; 15:815–823. [PubMed: 25137456]
36. Moon JJ, et al. Quantitative impact of thymic selection on Foxp3+ and Foxp3- subsets of self-peptide/MHC class II-specific CD4+ T cells. Proc Natl Acad Sci U S A. 2011; 108:14602–14607. [PubMed: 21873213]
37. Yu W, et al. Clonal Deletion Prunes but Does Not Eliminate Self-Specific alphabeta CD8(+) T Lymphocytes. Immunity. 2015; 42:929–941. [PubMed: 25992863]
38. Rizzuto GA, et al. Self-antigen-specific CD8+ T cell precursor frequency determines the quality of the antitumor immune response. The Journal of experimental medicine. 2009; 206:849–866. [PubMed: 19332877]
39. Walker LS, Abbas AK. The enemy within: keeping self-reactive T cells at bay in the periphery. Nature reviews. Immunology. 2002; 2:11–19.
40. Abadie V, Sollid LM, Barreiro LB, Jabri B. Integration of genetic and immunological insights into a model of celiac disease pathogenesis. Annu Rev Immunol. 2011; 29:493–525. [PubMed: 21219178]
41. Vader W, et al. The HLA-DQ2 gene dose effect in celiac disease is directly related to the magnitude and breadth of gluten-specific T cell responses. Proc Natl Acad Sci U S A. 2003; 100:12390–12395. [PubMed: 14530392]
42. Ito Y, et al. Detection of T cell responses to a ubiquitous cellular protein in autoimmune disease. Science. 2014; 346:363–368. [PubMed: 25324392]
43. Klein L, Kyewski B, Allen PM, Hogquist KA. Positive and negative selection of the T cell repertoire: what thymocytes see (and don't see). Nature reviews. Immunology. 2014; 14:377–391.
44. Burkett PR, Meyer zu Horste G, Kuchroo VK. Pouring fuel on the fire: Th17 cells, the environment, and autoimmunity. J Clin Invest. 2015; 125:2211–2219. [PubMed: 25961452]
45. Ghoreschi K, Laurence A, Yang XP, Hirahara K, O'Shea JJ. T helper 17 cell heterogeneity and pathogenicity in autoimmune disease. Trends Immunol. 2011; 32:395–401. [PubMed: 21782512]
46. Kleinewietfeld M, Hafler DA. The plasticity of human Treg and Th17 cells and its role in autoimmunity. Semin Immunol. 2013; 25:305–312. [PubMed: 24211039]
47. Gurung P, et al. FADD and caspase-8 mediate priming and activation of the canonical and noncanonical Nlrp3 inflammasomes. J Immunol. 2014; 192:1835–1846. [PubMed: 24453255]

48. Legoux FP, et al. CD4+ T Cell Tolerance to Tissue-Restricted Self Antigens Is Mediated by Antigen-Specific Regulatory T Cells Rather Than Deletion. Immunity. 2015; 43:896–908. [PubMed: 26572061]

49. Hirota K, et al. Plasticity of Th17 cells in Peyer's patches is responsible for the induction of T cell-dependent IgA responses. Nat Immunol. 2013; 14:372–379. [PubMed: 23475182]

50. Kazemi-Shirazi L, et al. IgA autoreactivity: a feature common to inflammatory bowel and connective tissue diseases. Clinical and experimental immunology. 2002; 128:102–109. [PubMed: 11982597]

Methods References

51. Viret C, Janeway CA Jr. Functional and phenotypic evidence for presentation of E alpha 52-68 structurally related self-peptide(s) in I-E alpha-deficient mice. J Immunol. 2000; 164:4627–4634. [PubMed: 10779766]

52. Nagai T, Abe A, Sasakawa C. Targeting of enteropathogenic Escherichia coli EspF to host mitochondria is essential for bacterial pathogenesis: critical role of the 16th leucine residue in EspF. J Biol Chem. 2005; 280:2998–3011. [PubMed: 15533930]

53. Nougayrede JP, Donnenberg MS. Enteropathogenic Escherichia coli EspF is targeted to mitochondria and is required to initiate the mitochondrial death pathway. Cell Microbiol. 2004; 6:1097–1111. [PubMed: 15469437]

54. Vallance BA, Deng W, Jacobson K, Finlay BB. Host susceptibility to the attaching and effacing bacterial pathogen Citrobacter rodentium. Infect Immun. 2003; 71:3443–3453. [PubMed: 12761129]

55. Sham HP, et al. Attaching and effacing bacterial effector NleC suppresses epithelial inflammatory responses by inhibiting NF-kappaB and p38 mitogen-activated protein kinase activation. Infect Immun. 2011; 79:3552–3562. [PubMed: 21746856]

56. Choi KH, et al. A Tn7-based broad-range bacterial cloning and expression system. Nat Methods. 2005; 2:443–448. [PubMed: 15908923]

57. Ferrieres L, et al. Silent mischief: bacteriophage Mu insertions contaminate products of Escherichia coli random mutagenesis performed using suicidal transposon delivery plasmids mobilized by broad-host-range RP4 conjugative machinery. J Bacteriol. 2010; 192:6418–6427. [PubMed: 20935093]

58. Ding Y, Shen S, Lino AC, Curotto de Lafaille MA, Lafaille JJ. Beta-catenin stabilization extends regulatory T cell survival and induces anergy in nonregulatory T cells. Nat Med. 2008; 14:162–169. [PubMed: 18246080]

59. Powrie F, Carlino J, Leach MW, Mauze S, Coffman RL. A critical role for transforming growth factor-beta but not interleukin 4 in the suppression of T helper type 1-mediated colitis by CD45RB(low) CD4+ T cells. The Journal of experimental medicine. 1996; 183:2669–2674. [PubMed: 8676088]

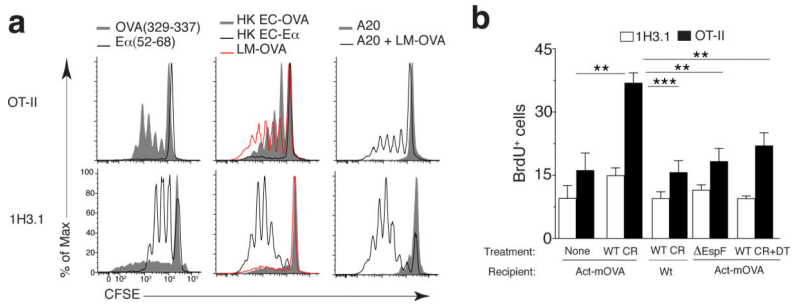

Figure 1. Presentation of apoptotic-cell-derived antigens during infection

(**a**) Proliferation of OT-II and 1H3.1 $CD4^+$ T cells (left margin) in response to BMDCs pulsed with OVA(329–337) or Eα(52–69) (left), phagocytosis of recombinant heat-killed *E. coli* expressing OVA (HK EC-OVA) or Eα (HK EC-Eα) or LM-OVA (middle), or phagocytosis of uninfected $Eα^+$ A20 cells (A20) or LM-OVA-infected apoptotic $Eα^+$ A20 cells (A20 + LM-OVA) (right), presented as dilution of the division-tracking dye CFSE. (**b**) Frequency of proliferating ($BrdU^+$) LI LP cells in Act-mOVA host mice given CD11c-DTR bone marrow and OT-II T cells plus 1H3.1 T cells and left uninfected (None) (n = 6) or infected with wild-type *C. rodentium* (WT CR) (n = 7), in wild-type host mice given bone marrow and T cells as above and infected with wild-type *C. rodentium* (n = 6), or in Act-mOVA host mice given bone marrow and T cells as above and infected with ΔEspF *C. rodentium* (n = 9) or infected with wild-type *C. rodentium* and treated with diphtheria toxin (WT CR+DT) (n = 6), assessed by flow cytometry with gating on $Vβ6^+$ (1H3.1) $CD4^+$ T cells or $Vα2^{hi}Vβ5^+$ (OT-II) $CD4^+$ T cells. $*P \leq 0.01$ and $**P \leq 0.001$ (one-way analysis of variance (ANOVA) and Tukey's post-test). Data are representative of three experiments (mean + s.d. in b).

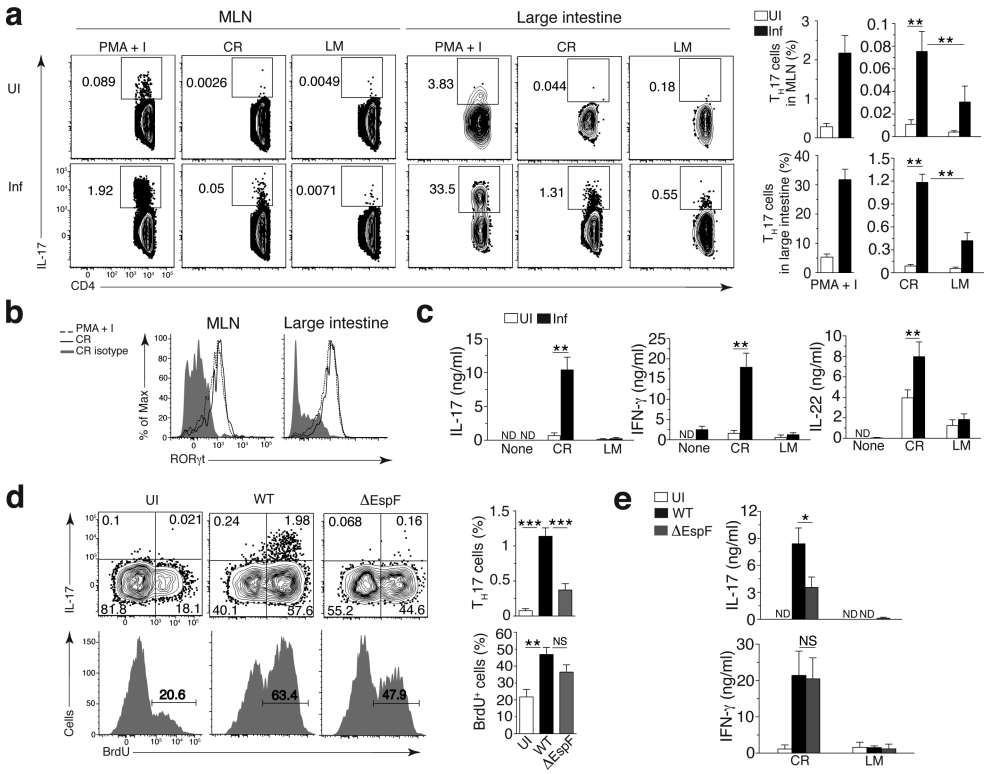

Figure 2. A *C. rodentium*-specific T_H17 response after orogastric infection with *C. rodentium*

(**a**) Flow cytometry (left) of $CD4^+$ T cells obtained from the MLNs and LI LP (top) of uninfected C57BL/6J mice (UI) or C57BL/6J mice at day 9 after infection with wild-type *C. rodentium* (Inf) (left margin), gated by flow cytometry on $Aqua^-B220^-CD45.2^+CD3^+$cells, followed by stimulation with PMA plus ionomycin (PMA+I) or with splenocytes pulsed with lysates of *C. rodentium* (CR) or Listeria monocytogenes (LM) (above plots). Numbers adjacent to outlined areas indicate percent $IL\text{-}17^+CD4^+$ (T_H17) cells. Right, quantification of results at left (n = 9 mice). (**b**) RORγt expression by $IL\text{-}17^+CD4^+$ T cells obtained from the MLNs or LI LP of mice (n = 5) infected and treated as in a (key), assessed by flow cytometry. (**c**) ELISA of IL-17, IFN-γ and IL-22 in supernatants of $CD4^+$ T cells obtained from the MLNs of uninfected mice or mice infected with wild-type *C. rodentium* (n = 12) and left unstimulated (None) or re-stimulated *ex vivo* with pathogen-pulsed splenocytes as in a (horizontal axes). (**d**) Flow cytometry (left) analyzing the IL-17 production (top) and proliferation (bottom) of $CD4^+$ T cells (gated as in **a**) from the LI LP of C57BL/6J mice left uninfected or at day 9 after infection with wild-type or ΔEspF *C. rodentium* (key). Numbers in quadrants (top) indicate percent cells in each (throughout); numbers above bracketed lines (bottom) indicate percent $BrdU^+$ (proliferated) cells. Right, quantification of the results at left, for uninfected mice (n = 7) or mice infected with wild-type *C. rodentium* (n = 9) or ΔEspF *C. rodentium* (n = 8). (**e**) ELISA of IL-17 and IFN-γ in supernatants of $CD4^+$ T cells obtained from the MLNs of mice left uninfected (n = 9) or infected with wild-type *C. rodentium* (n = 9) or ΔEspF *C. rodentium* (n = 9 (IL-17) or n = 12 (IFN-γ)) (key) and re-stimulated *ex vivo* with pathogen-pulsed splenocytes as in a (horizontal axes). ND, not detected. NS, not significant ($P > 0.05$); $*P \leq 0.05$, $**P \leq 0.01$ and $***P \leq 0.001$ (one-way ANOVA and Dunnet's post-test (**a**), one-way ANOVA and Tukey's post-test (**d**) or Mann-

Whitney test (**c,e**)). Data are representative of three independent experiments (**a,d**; mean + s.d.), two independent experiments (**b**) or four experiments (**c,e**; mean + s.d.).

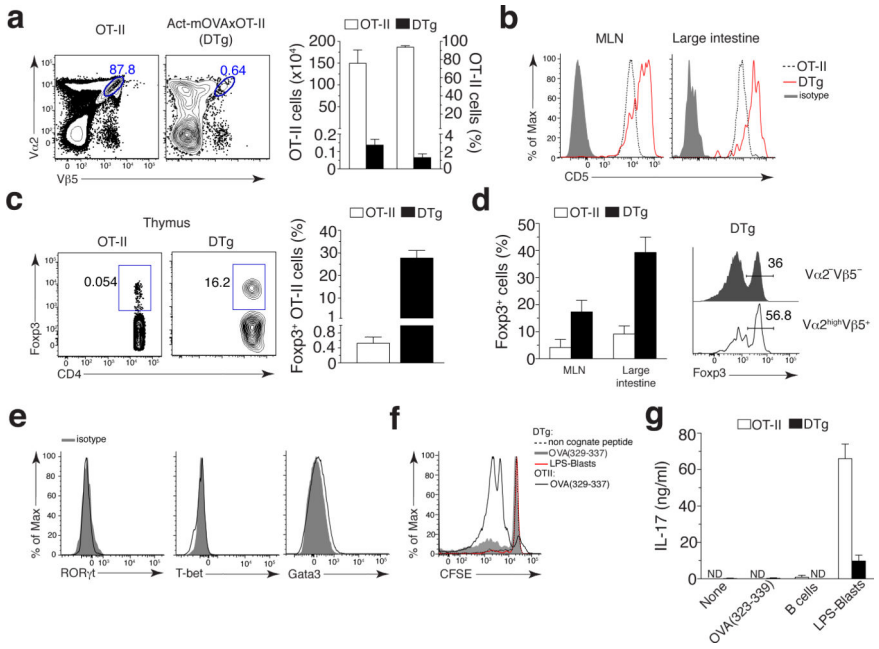

Figure 3. Detection of self-reactive CD4$^+$ T cells without an effector phenotype in DTg mice

(**a**) Frequency (**left**; numbers adjacent to blue outlined areas), and absolute number (middle) and frequency (**right**) of Vα2^{hi}Vβ5$^+$ CD4$^+$ T cells in the thymus of OT-II and DTg mice. (**b**) CD5 expression on I-A^b–OVA(328–337) tetramer–positive CD4$^+$ T cells from the MLNs and LI LP of OT-II and DTg mice. Isotype, isotope-matched control antibody. (**c**) Flow cytometry (**left**) of CD45$^+$CD8$^-$Vα2$^+$Vβ5$^+$ CD4$^+$ T cells from the thymus of OT-II and DTg mice. Numbers adjacent to outlined areas indicate percent Foxp3$^+$CD4$^+$ T cells. Right, frequency of Foxp3$^+$Vα2$^+$Vβ5$^+$ CD4$^+$ T cells in the thymus of OT-II or DTg mice. (**d**) Frequency of Foxp3$^+$Vα2$^+$Vβ5$^+$ CD4$^+$ T cells in the LI LP of OT-II and DTg mice (**left**), and flow cytometry of Vα2$^-$Vβ5$^-$ or Vα2^{hi}Vβ5$^+$ CD4$^+$ T cells (**right** margin) from the LI LP of the DTg mice at **left** (**right**). Numbers above bracketed lines (**right**) indicate percent Foxp3$^+$ cells. (**e**) Expression of RORγt, T-bet and GATA-3 in Vα2^{hi}Vβ5$^+$ LI LP CD4$^+$ T cells from uninfected DTg mice, assessed by flow cytometry. (**f**) Proliferation (CFSE dilution) of splenic CD25$^-$CD4$^+$ T cells from OT-II or DTg mice (key) after 5 d of culture with BMDCs pulsed with non-cognate peptide or OVA(329–337) (each at 10 μg/ml) or with BMDCs that had phagocytosed LPS-stimulated (LPS-blasts) apoptotic B cells isolated from Act-mOVA BALB/c mice. (**g**) Secretion of IL-17 by splenic T cells as in f, as well as T cells stimulated with BMDCs that had phagocytosed unstimulated apoptotic B cells from Act-mOVA BALB/c mice (B cells), assessed after 48 h of secondary re-stimulation with OVA(329–337). Data are representative of two independent experiments (**a–c, d, right, e–g**; mean + s.d. in **a,c,d,g**) with n = 5 (**a–c** and **d, right**) or n = 4 (**e**) mice, or three independent experiments with n = 9 mice (**d, left**; mean + s.d.).

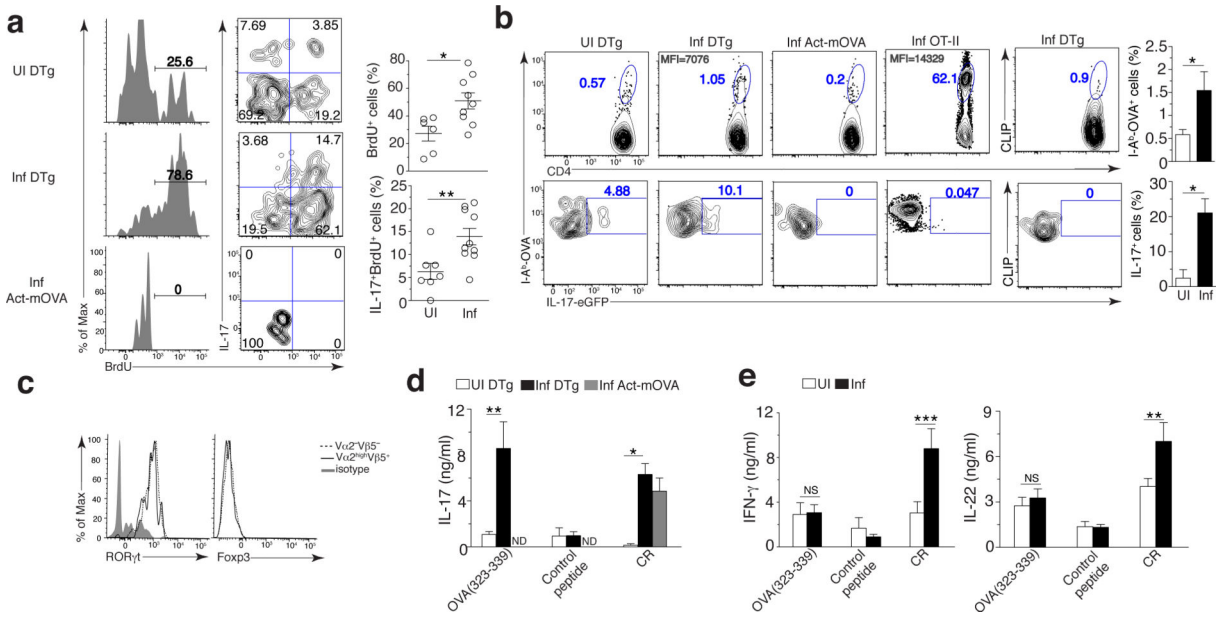

Figure 4. Infection promotes the proliferation of self-reactive CD4$^+$ T cells and their commitment to the T_H17 lineage

(**a,b**) Proliferation (**left**) and IL-17 production (**middle**) of LI LP Vα2^{hi}Vβ5$^+$CD4$^+$ T cells (gated on live B220$^-$CD45$^+$CD3$^+$CD4$^+$ cells) in DTg or Act-mOVA mice left uninfected or at day 9 after infection with *C. rodentium* (**left** margin; numbers above bracketed lines (**left**), as in Fig. 2d). Right, quantification of results at left: each symbol represents an individual mouse; small horizontal lines indicate the mean (± s.d.). (**b**) Flow cytometry (**left**) of CD4$^+$ T cells (gated as in a) from the LI LP of DTg, Act-mOVA or OT-II IL-17A–eGFP mice infected as in a, re-stimulated *ex vivo* with PMA plus ionomycin. Numbers adjacent to outlined areas indicate percent I-A^b–OVA tetramer–positive and IL-17A–eGFP$^+$ cells (**left** four columns) or CLIP (unrelated tetramer)–positive IL-17A–eGFP$^+$ cells (**right** column); numbers in top left corners indicate mean fluorescence intensity (MFI) of IL-17A–eGFP in the cells outlined. Far right, quantification of results at left. (**c**) Expression of RORγt and Foxp3 by various subsets (key) of IL-17$^+$CD4$^+$ T cells (gated as in a) from DTg mice at day 9 after infection with *C. rodentium*, assessed by flow cytometry. (**d,e**) ELISA of IL-17 (**d**) or IFN-γ and IL-22 (**e**) in supernatants of CD4$^+$ T cells from the MLNs of mice as in a (**d**) or DTg mice treated as in a (**e**) (key), re-stimulated *ex vivo* with OVA(323–339), a control peptide or *C. rodentium* (horizontal axis). *$P \leq 0.05$, **$P \leq 0.01$ and ***$P \leq 0.001$ (t-test (**a**), Mann-Whitney U test (**b**), one-way ANOVA and Dunnet's post-test (**d,e**) or Tukey's post-test (**e**, IL-22)). Data are representative of three (**a,c–e**) or two (**b**) experiments (mean and s.d.) with n = 7 mice (UI) or n = 10 mice (Inf) (**a,e**), n = 6 mice (**b**), n = 9 mice (**c**), or n = 6 mice (UI) or n = 8 mice (Inf) (**d**).

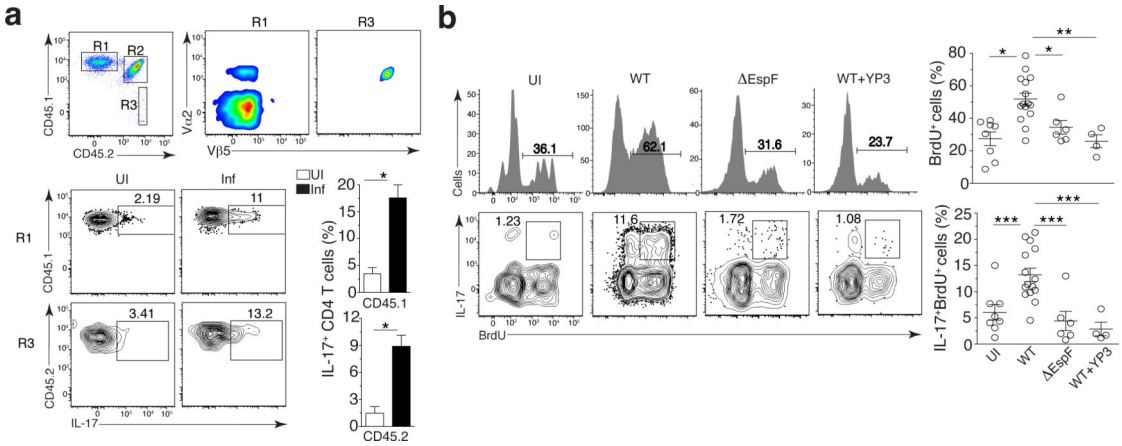

Figure 5. Apoptosis and self-antigen presentation are necessary for the activation of self-reactive T cells

(**a**) Flow cytometry of $CD4^+$ T cells (gated on $Aqua^-B220^-CD3^+$ cells) from the LI LP of uninfected Act-mOVA ($CD45.1^+CD45.2^+$) chimeras reconstituted with bone marrow from OT-II *Tcr*α$^{-/-}$ ($CD45.2^+$) mice and wild-type ($CD45.1^+$) mice (top row), and of wild-type (R1) and *Tcr*α$^{-/-}$ (R3) OT-II $CD4^+$ T cells (left margin) from chimeras left uninfected or at day 9 after infection with *C. rodentium* (above plots) (bottom left group). Outlined areas (top left) indicate wild-type (R1), endogenous (R2) and *Tcr*α$^{-/-}$ (R3) OT-II $CD4^+$ T cell populations; numbers adjacent to outlined areas (bottom left group) indicate percent $IL\text{-}17^+$ cells among $CD45.1^+$ or $CD45.2^+$ $CD4^+$ T cells. Bottom right, quantification of results at left. (**b**) Flow cytometry (left) of $V\alpha2^{hi}V\beta5^+$ $CD4^+$ T cells (gated on $Aqua^-B220^-CD45^+CD3^+$ cells) from the LI LP of DTg mice left uninfected or at day 9 after infection with wild-type or ΔEspF *C. rodentium* alone or infection with wild-type *C. rodentium* plus treatment with antibody to MHC class II (WT + Y3P) (above plots), followed by re-stimulation *ex vivo* with PMA plus ionomycin. Numbers above bracketed lines (top) indicate percent $BrdU^+$ (proliferated) cells; numbers adjacent to outlined areas (bottom) indicate percent $IL\text{-}17^+BrdU^+$ cells. Right, quantification of results at left: each symbol represents an individual mouse; small horizontal lines indicate the mean (± s.d.). $*P \leq 0.05$, $**P \leq 0.01$ and $***P \leq 0.001$ (t-test (**b**) or one-way ANOVA with Tukey's post-test (**c**)). Data are representative of three experiments with n = 7 mice (**a**) or three independent experiments with n = 8 mice (UI) , n = 15 mice (WT), n = 6 mice (ΔEspF) or two independent experiments with n = 4 mice (wild-type + YP3) (**b**).

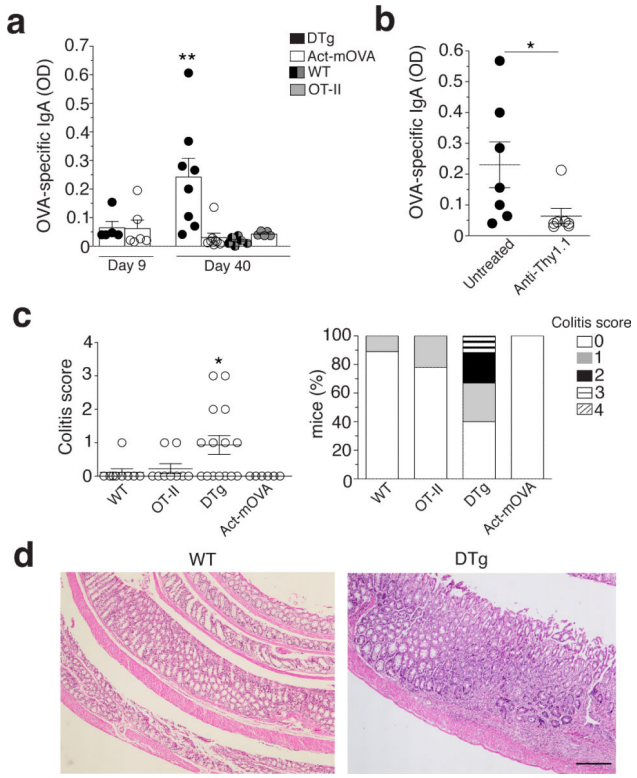

Figure 6. The generation of self-reactive T_H17 cells is associated with a self-reactive IgA response and intestinal pathology

(**a**) Quantification of anti-OVA IgA in the serum of DTg, Act-mOVA, wild-type and OT-II mice (key) on days 9 and 40 after infection with *C. rodentium* (horizontal axis), presented as absorbance at 490 nm (A490). (**b**) Quantification of anti- OVA IgA in Act-mOVA chimeras (n = 7) reconstituted with bone marrow from wild-type and OT-II mice and infected with *C. rodentium*, then left untreated or depleted of OT-II T cells with anti-Thy1.1 (horizontal axis; **Supplementary Fig. 6b**), assessed on day 40 after infection (presented as in **a**). (**c**) Colitis scores (left) of wild-type, OT-II, DTg and Act-mOVA mice on day 40 after infection with *C. rodentium* (on a scale of 0 (no change) to 4 (most severe) for inflammation, crypt abscesses, granulomatous inflammation, hyperplasia, mucin depletion, ulceration and crypt loss), and frequency of such mice with each score (right). (**d**) Hematoxylin-and- eosin staining of sections of large intestine from wild-type and DTg mice on day 40 after infection with *C. rodentium*. Scale bar, 250 μm. Each symbol (**a,b,c**) represents an individual mouse; small horizontal lines (**b,c**) indicate the mean (± s.d.). $*P \leq 0.05$ and $**P \leq 0.01$ (one-way ANOVA and Dunnet's post-test (**a,c**) or t-test (**b**)). Data are representative of three experiments with n = 6 mice (DTg and Act-mOVA at day 9; wild-type and OT-II at day 40) or n = 8 mice (DTg and Act-mOVA at day 40) (**a**; mean + s.d.), two experiments (**b**) or three experiments with n = 6 mice (Act- mOVA), n = 9 mice (wild-type and OT-II) or n = 15 mice (DTg) (**c,d**).